Temperature dependence of the shear modulus of soft tissues assessed by ultrasound

2010 Phys. Med. Biol. 55 1701

(http://iopscience.iop.org/0031-9155/55/6/011)

IOP PUBLISHING PHYSICS IN MEDICINE AND BIOLOGY

Phys. Med. Biol. **55** (2010) 1701–1718 doi:10.1088/0031-9155/55/6/011

Temperature dependence of the shear modulus of soft tissues assessed by ultrasound

E Sapin-de Brosses[1], **J-L Gennisson, M Pernot, M Fink and M Tanter**

Langevin Institute (CNRS UMR 7587), INSERM ERL U979, ESPCI ParisTech,
10 rue Vauquelin, 75 005 Paris, France

E-mail: emilie.sapin@espci.fr

Received 16 November 2009, in final form 29 January 2010
Published 2 March 2010
Online at stacks.iop.org/PMB/55/1701

Abstract

Soft tissue stiffness was shown to significantly change after thermal ablation. To better understand this phenomenon, the study aims (1) to quantify and explain the temperature dependence of soft tissue stiffness for different organs, (2) to investigate the potential relationship between stiffness changes and thermal dose and (3) to study the reversibility or irreversibility of stiffness changes. *Ex vivo* bovine liver and muscle samples ($N = 3$ and $N = 20$, respectively) were slowly heated and cooled down into a thermally controlled saline bath. Temperatures were assessed by thermocouples. Sample stiffness (shear modulus) was provided by the quantitative supersonic shear imaging technique. Changes in liver stiffness are observed only after 45 °C. In contrast, between 25 °C and 65 °C, muscle stiffness varies in four successive steps that are consistent with the thermally induced proteins denaturation reported in the literature. After a 6 h long heating and cooling process, the final muscle stiffness can be either smaller or bigger than the initial one, depending on the stiffness at the end of the heating. Another important result is that stiffness changes are linked to thermal dose. Given the high sensitivity of ultrasound to protein denaturation, this study gives promising prospects for the development of ultrasound-guided HIFU systems.

(Some figures in this article are in colour only in the electronic version)

1. Introduction

There has been increasing interest in high-intensity focused ultrasound (HIFU) for thermal ablation of tumors because this technique can non-invasively treat small and deep targets without injury to the surrounding tissue. However, there are currently few methods for

[1] Author to whom any correspondence should be addressed.

real-time monitoring of the therapy. Direct assessment of the temperature has been proposed using magnetic resonance imaging (MRI). Thanks to the ability of MR to provide temperature maps with good accuracy every few seconds, this technique has been implemented clinically and used successfully for the treatment of uterine fibroids (Cline *et al* 1994, Rieke and Pauly 2008). This approach is to date considered as the 'gold standard' for the monitoring of HIFU treatments as it provides an experimental way to assess temperature elevation and the cumulative thermal dose. However, MR thermometry is not totally free of drawbacks. Although it is unavoidable for high precision applications such as brain therapy, the clinical use of MRI is limited by its cost, in particular for applications such as liver RF ablation or other common thermal ablation treatments.

Parallel to MR thermometry, ultrasound-based methods were proposed to map temperature elevation in tissues. All these approaches are based on changes in acoustical properties (speed of sound or attenuation). Ultrasound-based thermometry (Anan and Kaczkowski 2008, Curiel *et al* 2009, Maass-Moreno *et al* 1996, Miller *et al* 2002, Pernot *et al* 2004, Seip and Ebbini 1995, Simon *et al* 1998) has been proven to detect *in vitro* HIFU lesions, but it still suffers limitations that should be overcome to be usable in practical *in vivo* clinical conditions. Two limitations are currently limiting its dissemination. First, this approach is extremely sensitive to motion artifacts: the general concept for temperature changes estimation lies in the assessment of apparent tissue displacements due to sound speed changes and thermal expansion. Second, the temperature dependence of sound speed is very small (typically $1\ \mathrm{m\,s^{-1}\,{}^{\circ}C^{-1}}$) as it is mainly due, in the 37–50 °C range, to the temperature dependence of the bulk modulus K. It results in very small apparent tissue displacements of a few microns.

However, the mechanical behavior of human tissue is not only characterized by the bulk modulus K (inverse of the compressibility $\kappa = 1/K$) but also by the shear modulus μ. K is almost uniform (less than 5% fluctuations) in all soft tissues with typical values of ∼1 GPa. Moreover, K does not change significantly with pathology or temperature changes, as it is defined mainly by molecular composition of tissue and short range molecular interaction. Since most soft tissues are about 80% made of water, it is not much different from the water bulk modulus. In contrast, μ is very small with typical values of some kPa and it strongly varies from one organ to the other. Bulk and shear moduli are directly linked to stiffness characterized by Young's modulus E via the relationship

$$E = \frac{9K\mu}{3K + \mu}. \tag{1}$$

Soft human tissues are mainly characterized by the fact that K is huge in comparison with μ. This property is a kind of definition of 'soft solids' and human soft tissues belong to this category. It straightforwardly implies a well-known link between stiffness E and the shear modulus μ: $E = 3\mu$. μ is defined by cellular but also interestingly by higher levels of structural organization of tissue, and consequently, it can be greatly affected by pathological or physiological changes in tissue structure. As it strongly affects the tissue structure, thermal necrosis of a soft tissue should result in a dramatic change of tissue shear modulus.

Therefore, another approach for HIFU treatment monitoring consists in the assessment of lesion stiffness changes with temperature. This hypothesis was verified by Ophir *et al* (1991) using static elastography. In their study, local strain was found to be significantly smaller in thermally ablated lesions than in surrounding untreated tissues. 2D elastograms (images of local tissue strain) were performed during a static compression and revealed the shape of the ablated region.

In 2004, Bercoff *et al* (2004b) proposed to use the supersonic shear imaging technique for the quantitative and real-time imaging of tissue stiffness. Supersonic shear imaging (SSI) is an ultrasound-based technique that provides quantitative shear modulus mapping of soft

media. The basic principles of the method were previously described (Bercoff *et al* 2004b, Muller *et al* 2009, Tanter *et al* 2008). Briefly, an acoustic radiation force is remotely induced in tissue using a short ($\sim$100 μs) burst of focused ultrasound to create a low-frequency shear wave in the medium. Then, images of the propagation of the resulting transient shear waves are made at an ultrahigh frame rate (up to 10 000 images s^{-1}), from which the elasticity map is recovered by solving a local inverse problem. This method was applied for the diagnosis of breast cancer (Tanter *et al* 2008) and for the assessment of liver or muscle stiffness (Muller *et al* 2009). Furthermore, the potential interest of this quantitative method for thermal necrosis was evaluated by Bercoff *et al* (2004a). The SSI approach was found to be able to image the quantitative stiffness of *in vitro* HIFU ablated regions and exhibit three to four times stiffer values in the post-treatment lesions. However, beyond such 'proof of concept' experiments, there is a real need to better explain the temperature dependence of stiffness in order to understand if stiffness changes could be a reliable parameter for the control of tissue damages induced by thermal ablation.

The temperature dependence of the Young's modulus of soft tissues was revealed by Apter (1972). The collagen denaturation was responsible for irreversible stiffness changes; with increasing temperature, collagen fibers gain enough energy to overcome the state of an irreversible transformation from a helical-ordered state to a random-like structure (Lepetit *et al* 2000, Wall *et al* 1999, Wright and Humphrey 2002). This transformation is assumed to begin at about 60 °C (Lepetit *et al* 2000, Wall *et al* 1999, Wright and Humphrey 2002). The thermomechanics of one collagen fiber follows an Arrhenius equation. However, at the tissue level, there is currently no globally accepted thermomechanical model that describes the changes of the shear modulus with temperature because of the complex interactions between fibers (Lepetit *et al* 2000, Lepetit 2007). The most complete study was conducted by Wu *et al* (2001) who had identified three patterns: (1) a reversible decrease of the shear modulus with increasing temperature between 20 °C and 60 °C, (2) an irreversible increase around 60 °C corresponding to the threshold of denaturation and (3) a reversible increase of the shear modulus during cooling for tissues that undergone an irreversible thermal damage. These patterns have been observed using magnetic resonance elastography, which has the limitations of MRI.

It has been shown by Sapareto and Dewey (1984) that cellular death is linked to the history of heating, i.e. linked to temperature and time, via the so-called thermal dose. This empirical definition is widely used in ultrasonic thermal ablation and hyperthermia. Of particular interest could be the relationship between thermal dose and the changes of tissue stiffness during heating, which reflects both cellular and macro level tissue structural changes.

Hence, the study first aims to quantify and explain the temperature dependence of the shear modulus of both isotropic and anisotropic *ex vivo* tissues (bovine liver and bovine muscle, respectively). Second, taking benefit of the quantitative assessment of tissue stiffness provided by SSI, this article aims to investigate the potential relationship between elasticity changes and thermal dose. Third, it aims to study the reversibility or irreversibility of the thermal effects on *ex vivo* tissue mechanical properties.

2. Material and methods

2.1. Specimens

Three samples from 1 bovine liver (from butcher shop) and 19 samples from 14 bovine muscles (rump roast beef from a butcher shop) were considered. The samples were pseudo-parallelepipeds whose dimensions ranged between $80 \times 40 \times 20$ and $100 \times 90 \times 50\,mm^3$. One

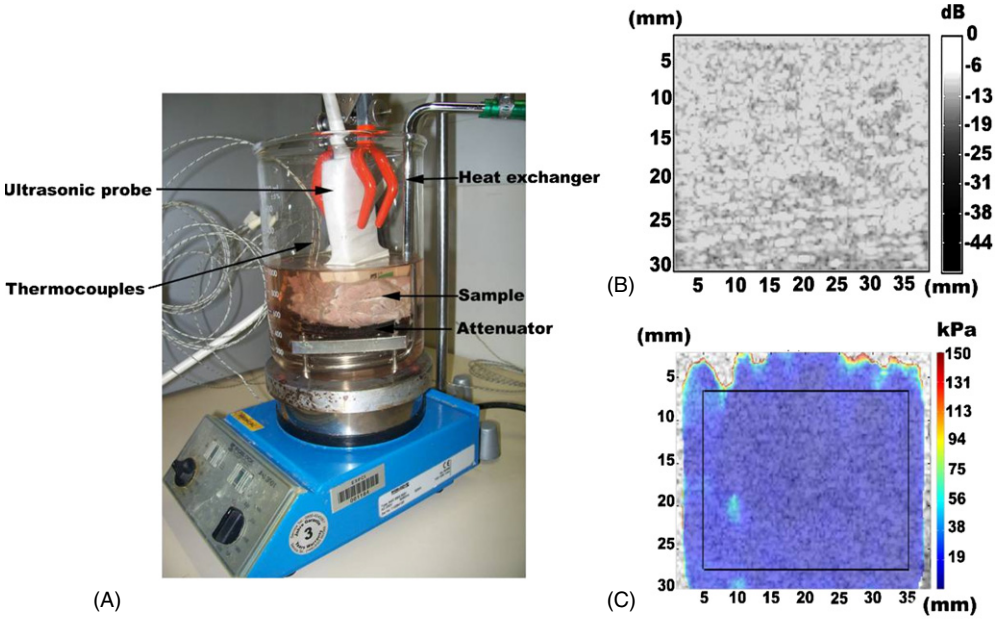

Figure 1. (A) Experimental set up. (B) Typical B-mode image. (C) Typical stiffness map and region of interest chosen for the shear modulus calculation.

liver sample was tested the day it was bought, and the two others were tested 48 h later. The muscular specimens were tested the day they were bought or at most the day after. Information about the preservation of the tissue was not available. Specimens were not degassed.

2.2. *Temperature assessment*

The samples were slowly warmed up and cooled down into a thermally controlled saline bath (figure 1(A)) (thermal unit: Ministat 125, Hueber). Three thermocouples (type J, accuracy = 1.5 °C), connected to a multichannel acquisition board (Sensoray Model 7409TB), were used to assess temperatures every minute. One thermocouple was placed into the bath, and the two others were placed into the bovine samples at two distant points. The temperature distribution was quite homogeneous (variance of temperature within the sample less than 2 °C). In the following, the temperature within the sample is the average of the two measures.

2.3. *Supersonic shear imaging sequence*

Local stiffness was assessed using a conventional ultrasonic probe (L7-4, ATL, Seattle, USA) with 128 elements at 5 MHz central frequency and 0.3 mm pitch, driven by an ultrasound research system (V1, Supersonic Imagine, Aix-en-Provence, France). By successively focusing the ultrasonic 'pushing' beam for 200 μs at different depths (7, 14, 21 and 28 mm), a supersonic shear source, which moved faster than the shear waves, was created. All resulting shear waves interfered constructively along a Mach cone creating two quasi-plane shear wave fronts propagating in opposite directions. Then, images of the propagation of the resulting transient plane shear waves were made at 5000 frames s^{-1}. Indeed, as shear waves propagate

through the medium in a few tens of milliseconds, frame rates of a few kilohertz are needed to catch their propagation. Such a frame rate, not reachable with standard ultrasound devices, is possible with the SSI ultrafast scanner as it reduces the emitting mode to a single plane wave insonification. After the acquisition of radiofrequency signals at an ultrafast frame rate, the data were transferred to a computer and a beamforming algorithm applied to the data enabled to build final ultrasonic images as described in Bercoff *et al*'s study (2004b) (figure 1(B)). The axial displacements induced in soft tissues by the shear wave propagation were estimated by cross-correlating successive ultrasound images. Thanks to a time-of-flight algorithm, a map of the local shear group velocity was obtained. The resulting velocity field was a broadband spectrum centered on 150 Hz to 200 Hz depending on the sample, and a low pass filter at 400 Hz was used in order to improve the signal-to-noise ratio. Assuming the medium to be purely elastic, infinite, locally isotropic and homogeneous, a local and quantitative estimation of the shear modulus μ was made from the shear velocity (c_s) in the whole image region, except in the source zone, using the formula: $\mu = \rho c_S^2$, where the volumic mass ρ was assumed to be a constant and equal to 1000 kg m^{-3}.

Finally, three successive Mach cones were created at three different lateral positions (transducer numbers 32, 64, 96) to provide a stiffness map of the whole image region by combining the data (Tanter *et al* 2008) (figure 1(C)).

The stiffness mapping was achieved every minute. A region of interest (ROI) was chosen and the shear modulus of the sample was computed as the median of the local values in the ROI. A typical example is presented in figure 1(C).

2.4. Experiments

Four different cases were studied.

Case 1: Temperature dependence of the shear modulus. The aim of this part was to assess variations of the shear modulus with temperature for different organs. First, the three bovine liver samples were slowly heated at 67 °C (liver 1), 55 °C (liver 2) or 50 °C (liver 3) and then cooled back (temperature rate of 0.3 °C min^{-1}, total time to heat equal to 144 min, 120 min and 103 min, respectively). In the same time, stiffness maps were computed every minute. Second, seven samples extracted from seven different bovine muscles were slowly heated and cooled back. The saline bath was heated from 25 °C to 70 °C by steps of 10 °C high and 20 min long and then cooled back at room temperature following the same steps resulting in a temperature rate in the sample equal to 0.3 °C min^{-1}. Stiffness was assessed along the muscular fibers every minute ('longitudinal shear modulus').

Case 2: Influence of tissue anisotropy. To quantify the influence of tissue anisotropy, four samples, extracted from four out of the previous bovine muscles, were submitted to the same thermal conditions as in case 1, but stiffness was assessed perpendicularly to the muscular fibers ('transversal shear modulus').

Case 3: Stiffness irreversibility. To identify temperature thresholds above which stiffness changes are irreversible, four samples extracted from four different bovine muscles were submitted to successive heating-and-cooling cycles. The water was slowly heated from 25 °C to a targeted temperature, kept at this temperature for 20 min and cooled back at 25 °C for 20 min resulting in a temperature rate in the sample equal to 0.3 °C min^{-1}. This pattern was successively applied for the following targeted temperatures: 30 °C, 40 °C, 50 °C, 60 °C and 70 °C. In the same time, the longitudinal shear modulus was assessed every minute.

Case 4: Relationship between thermal dose and stiffness change. To study the combined effect of time and temperature, four samples extracted from three different bovine muscles were heated with temperature and time conditions corresponding to cumulative thermal doses about hundred times bigger than the threshold of cellular necrosis for muscle (240 min (Meshorer 1983)). The cumulative thermal dose was calculated as defined by Sapareto and Dewey (1984):

$$\mathrm{CEM}_{43^\circ\mathrm{C}}(t) = \sum_{t_i<t} R^{43-T(i)}(t_i - t_{i-1}) \tag{2}$$

where $T(i) = \frac{T_i+T_{i-1}}{2}$ is the average of the temperatures at the successive instants t_{i-1} and t_i and R is an empirical value that depends on the temperature ($R = 0$ for $T(i) < 39\ ^\circ$C, $R = 0.25$ for $39\ ^\circ\mathrm{C} < T(i) < 43\ ^\circ$C, $R = 0.5$ for $T(i) > 43\ ^\circ$C). In the same time, stiffness was assessed along muscular fibers.

2.5. *Effect of fluid transfers on tissue elasticity*

To explore if blood and fat loss as well as water perfusion in the sample bias or delay the thermal injury of the tissue, two samples extracted from one bovine muscle were heated and cooled down following the previous steps. One was placed directly into the saline bath as explained previously and the other was placed into a hermetic plastic box in order to avoid the transfer of fluids between the saline bath and the sample.

3. Results

3.1. *Reproducibility, spatial and inter-sample variances*

The standard deviation of the shear modulus, for five successive SSI assessments at 25 °C, was at most 2.1% of the measured value (table 1). According to this variability, elasticity changes higher than ± 2.1% should be due to other reasons than the SSI method.

The spatial standard deviation of the shear modulus in the ROI selected on the stiffness map (see figure 1(C)) was less than 1.2% for liver tissues and was in the 11–50% range for muscular tissues (table 1). This spatial variance was affected by temperature: it was slightly smaller at 50 °C than at 25 °C for most of the samples (table 1).

The average shear modulus of the three liver samples, before heating, was equal to 3.4 kPa. The average longitudinal shear modulus at 25 °C of the bovine muscles was equal to 78 kPa ($N = 7$ different muscles), whereas the average transversal shear modulus at 25 °C was equal to 33 kPa ($N = 4$ different muscles). The standard deviation of the spatially averaged shear modulus between different samples was called the inter-sample standard deviation. For the three liver samples, it was equal to ± 0.5 kPa, i.e. ± 15% of the mean value (table 1). The inter-sample standard deviation of the shear moduli of bovine muscles before heating was equal to ± 27 kPa (±35%) for measurements along the fibers and ± 21 kPa (± 63%) for measurements perpendicular to fibers (table 1). According to these huge variances, normalized values (shear modulus/shear modulus at 25 °C) are used below for muscular tissue.

Case 1: Temperature dependence of the shear modulus. Stiffness changes induced by heating were different for liver tissue and muscular tissue. The shear modulus of liver tissue was almost constant during heating up to 45 °C and then exponentially increased. While cooling back the samples, the shear modulus decreased for liver 1 (−16%) but increased for liver 2 and liver 3 (+36% and +74%, respectively; figure 2).

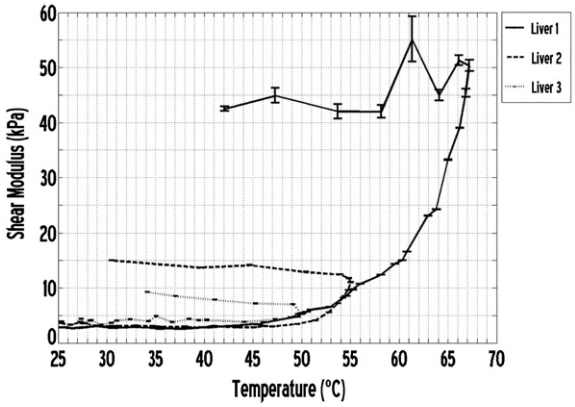

Figure 2. Evolution of the shear modulus with temperature for three samples extracted from one bovine liver. Error bars represent the spatial variance of the shear modulus in the ROI.

Table 1. Typical relative standard deviations of shear modulus at 25 °C and 50 °C. The standard deviation of the SSI assessment quantifies the reproducibility of the stiffness measurement for five successive estimates made before heating (at 25 °C). The standard deviation in the ROI quantifies the structural heterogeneity of the medium. Values are given at 25 °C and 50 °C. The inter-sample standard deviation quantifies the variability of the spatially averaged shear modulus between different samples. Values are given at 25 °C and 50 °C.

Sample		Relative standard deviation of the shear modulus				
		Of the SSI estimates	In the ROI		Between different samples	
			At 25 °C	At 50 °C	At 25 °C	At 50 °C
Liver	Liver 1	0.5%	1.2%	0.2%	15% $N = 3$	23% $N = 3$
	Liver 2	1.8%	0.3%	0.1%		
	Liver 3	0.2%	1.1%	0.6%		
Muscle Assessment along the fibers	Muscle 1	0.6%	20.6%	15.7%	35% $N = 7$	49% $N = 7$
	Muscle 2	1.4%	11.3%	23.4%		
	Muscle 3	2.1%	33.9%	34.3%		
Muscle Assessment perpendicular to the fibers	Muscle 1	0.6%	17.7%	46.1%	63% $N = 4$	51% $N = 4$
	Muscle 2	1.6%	49.5%	46.6%		
	Muscle 3	0.9%	38.7%	29.9%		
	Muscle 4	1.0%	40.2%	31.4%		

The shear modulus of muscular tissue changed by heating and four phases were identified: the normalized shear modulus linearly decreased with temperature up to 43 °C with a change of slope at about 37 °C (-2.5% °C^{-1} up to 37 °C and -2.0% °C^{-1} between 37 °C and 43 °C) and then it exponentially decreased up to 57 °C. Finally, it exponentially increased up to 64 °C (figure 3).

During cooling, the behavior depended on the ratio between the shear modulus at the end of heating and the shear modulus before heating (at 25 °C). If the ratio was superior to 0.86, the shear modulus increased during cooling (figure 4(A)) and the final stiffness was bigger

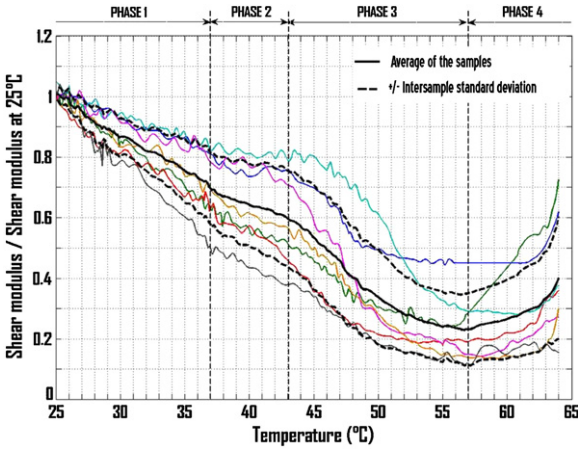

Figure 3. Evolution of the normalized shear modulus along the muscular fibers ('longitudinal shear modulus') during heating for seven bovine muscles. Four phases are identified: the shear modulus linearly decreases up to 43 °C with a change of slope at 37 °C (phases 1 and 2), then it exponentially decreases up to 57 °C (phase 3) and finally it exponentially increases until the end of the heating (phase 4).

than the initial one. If the ratio was smaller than 0.81, the shear modulus did not change during cooling and the medium was finally softened (figure 4(B)). To better explain this pattern, two additional experiments were made on two samples extracted from one muscle (different from the previous ones). One sample was heated up to 66 °C following the protocol described in section 2 and the other was heated and kept at 66 °C until the shear modulus reached 90% of the initial value at the end of the heating (it corresponded to heating for 50 min in this case). The shear modulus increased during cooling for the former sample, whereas it remained constant for the latter. No case was reported between 0.81 and 0.86. It should be noticed that, for all the cases, the stiffness changes were irreversible as the final stiffness was different from the initial value.

Case 2: Effects of anisotropy. The transversal shear modulus before heating (at 25 °C) was 1.80 ± 0.19 times smaller than the longitudinal shear modulus assessed on the same sample at 25 °C. The transversal shear modulus exhibited almost the same general behavior than the longitudinal shear modulus. However, contrary to the longitudinal shear modulus, only three phases were identified: the shear modulus linearly decreased up to 43 °C at a rate equal to $-2\%\ °C^{-1}$, then exponentially decreased up to 57 °C and finally exponentially increased with increasing temperature (figure 5). It should be noted that the temperature thresholds were the same as those identified for the longitudinal shear modulus. As previously noted for the longitudinal shear modulus, two cool down behaviors were observed depending on the shear modulus at the end of the heating.

Case 3: Reversibility–irreversibility of stiffness changes. The goal was here to identify a potential temperature threshold above which stiffness changes are irreversible. Four samples were submitted to successive warm up and cool down cycles, from 20 °C to 70 °C by steps of 10 °C high and 20 min long. For two out of the four samples, the shear modulus decreased when heating up to 62 °C and then returned to a value close to the initial shear modulus during

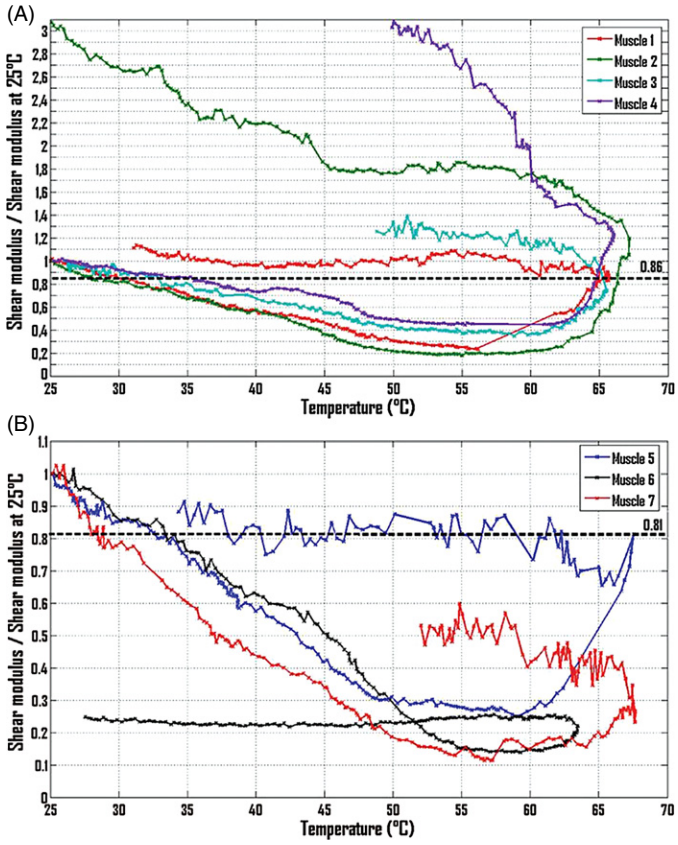

Figure 4. Evolution of the normalized shear modulus along the fibers during heating and cooling. (A) At the end of the heating, stiffness was bigger than 86% of the initial value: the shear modulus increased during cooling. (B) At the end of the heating, stiffness was smaller than 81% of the initial value: the shear modulus was quasi constant during cooling.

cooling (figure 6(A)). These changes were not linear and the heating curves were different from the cooling curves, which resulted in hysteresis loops. The coefficients driving the curves were the same up to 62 °C, but the area between the curves increased with increasing temperature. Above 62 °C, the shear modulus increased during cooling with a slope significantly bigger than the previous ones, and the final shear modulus was significantly different from the initial value (figure 6(A)). For the two other samples, hysteresis loops were observed up to 49 °C and the area between the curves increased with increasing temperature, but above 49 °C, the cooling curves significantly differed from the previous ones and there was no loop anymore: the shear moduli at the end of the heating-and-cooling cycles decreased and were different from the initial value. Above 62 °C, the shear modulus increased during heating and cooling (figure 6(B)).

Case 4: Relationship between tissue stiffness and thermal dose. Four samples were heated at different temperatures and different durations. The first sample was heated at 48 °C for 50 min, the second sample was heated at 50.5 °C for 70 min, the third one at 51.5 °C for 53 min and the last one was heated at 55 °C for 3 min. The cumulative thermal doses were equal to

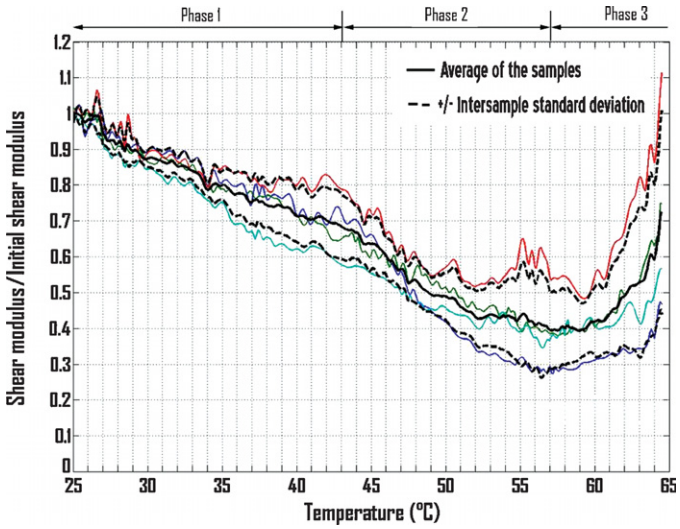

Figure 5. Evolution of the normalized shear modulus perpendicular to the muscular fibers ('transversal shear modulus') during heating for four bovine muscles. Three phases are identified: the shear modulus linearly decreases up to 43 °C (phase 1), then it exponentially decreases up to 57 °C (phase 2) and finally it exponentially increases until the end of the heating (phase 3).

2200, 20 000, 25 000, 49 000 min at 43 °C, respectively. The first sample should have been heated for 12 h to achieve a value close to the other thermal doses, but the size of the resulting data would be bigger than the capacity of the memory system. Because the thermal dose is defined for temperatures above 39 °C, the shear modulus was normalized by the value at 39 °C to allow comparison between the samples (figure 7).

The changes of the shear modulus with the thermal dose were the same for all the samples (figure 7). The normalized shear modulus linearly decreased with increasing thermal dose up to 20 min at a rate of -1.5% min^{-1}, then exponentially decreased up to 5000 min, and finally slowly decreased and even stabilized excepted for the 55 °C line.

3.2. Effect of fluid transfers on tissue elasticity

Blood and fat loss increased above 50 °C. Comparison between the sample heated in the saline bath with the one heated in the box showed that stiffness decreased at different rates between 25 °C and 43 °C (-0.01% °C^{-1} in water versus -0.02% °C^{-1} in the box). However, the difference was smaller than the spatial variance.

4. Discussion

In the context of thermal ablation of tumors, the prediction of *in vivo* heat-induced changes remains problematic. Hence, there is a need to better understand the effects of temperature on soft tissues stiffness.

The present study aimed (1) to quantify and explain the variations of the shear modulus of both isotropic and anisotropic tissues during controlled hyperthermia using the supersonic shear imaging (SSI) ultrasonic method, (2) to study the relationship between stiffness changes

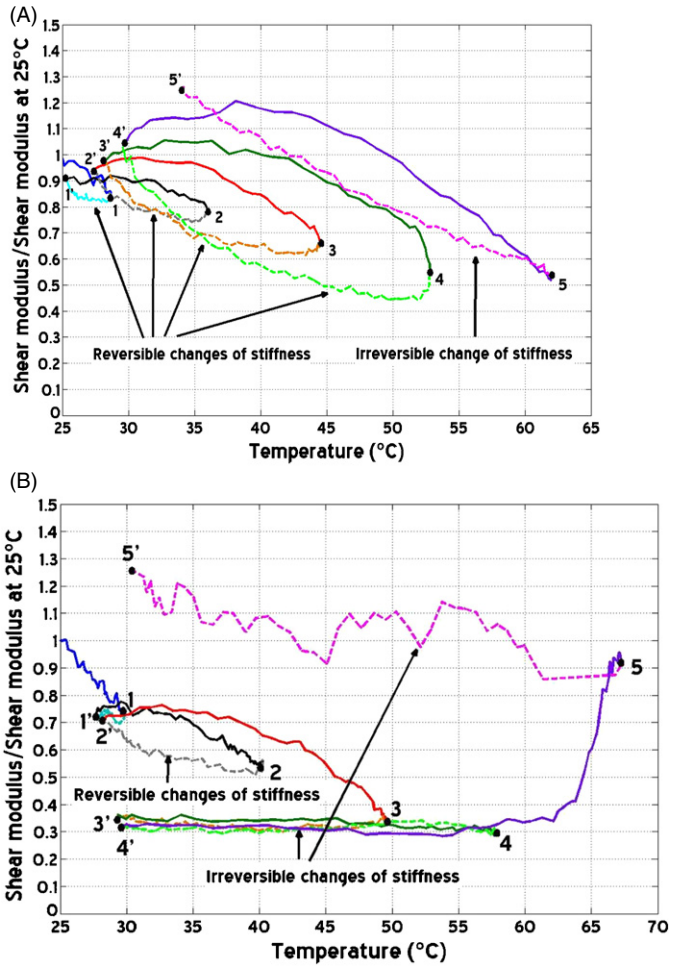

Figure 6. Evolution of the shear modulus for successive warm up and cool down cycles. Cycle number *i*: point number '*i*' is the end of heating, point number '*i*' ' is the end of cooling. Two different behaviors are observed: (A) the evolution of the shear modulus is quasi reversible up to 62 °C; (B) the evolution of the shear modulus is not reversible above 49 °C.

and thermal dose and (3) to identify temperature thresholds of irreversible stiffness changes, for further clinical applications.

4.1. Reproducibility, spatial and inter-sample variances

The variance of the SSI assessment was small enough (<2.1%) to provide a very accurate evaluation of local liver and muscle stiffness. This good reproducibility enables us to quantify stiffness heterogeneity in the image and small stiffness changes under thermal constraints.

The shear modulus of liver tissues before heating (at room temperature) was in the range of data reported in the literature (Kruse *et al* 2000, Kiss *et al* 2009). The spatial variance of the shear modulus into the region of interest was very small (<1.2%) showing that bovine liver is a quite homogeneous and isotropic medium. The inter-sample variance (samples extracted from the same liver in this case) was moderate (<23%) but much bigger than the spatial variance. The samples were not tested the same day, which could explain this variability.

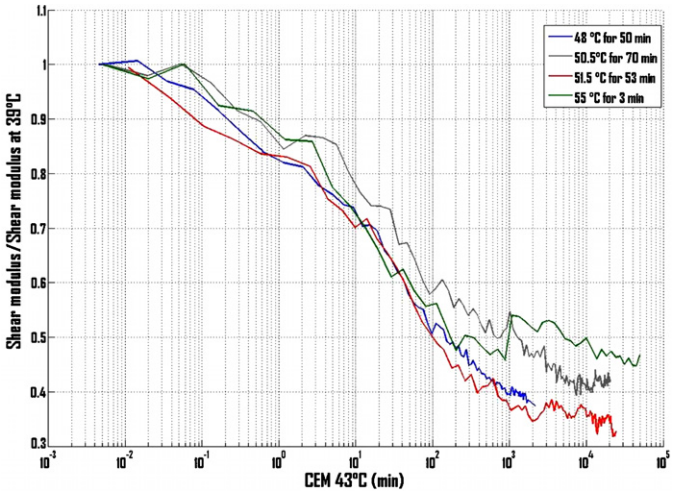

Figure 7. Combined influence of temperature and time for four bovine muscles: evolution of the shear modulus as a function of the cumulative thermal dose (CEM 43 °C)

The shear moduli of bovine muscular tissues assessed using SSI (between 17 kPa and 128 kPa) were bigger than previous values assessed using magnetic resonance elastography (between 20 kPa and 70 kPa) (Kruse *et al* 2000, Wu *et al* 2001). This is probably due to the variability of the mechanical properties between skeletal muscles due to the different anatomical location, the organization of the muscular fibers or fat infiltration. The high spatial variance of the shear modulus into the region of interest for muscular tissue (11–50%) was typical of a highly structured and heterogeneous medium. This spatial variability is not due to the variability of the method (<2.1%) but to anatomical reasons: the number, the orientation and the organization of the muscular fibers or fat quantity infiltrated are not homogeneous in a muscle, so that the shear modulus, linked to the muscular structure, is not the same for several samples extracted from different regions of the same muscle. Moreover, according to the inter-sample standard deviation of the shear modulus for muscular tissues (variance between samples extracted from different muscles in this case), normalized values were needed to compare the results between samples.

4.2. Temperature dependence of the shear modulus

Soft tissue stiffness is strongly affected by temperature changes. However, these dynamic variations differ from one organ to the other.

First, three samples extracted from one bovine liver were studied. During heating, their shear modulus was almost constant up to 45 °C and exponentially increased above 45 °C. The shear modulus decreased for one sample which was very stiff at the end of the heating phase, but increased for the two others (figure 2). However, the small number of liver specimens in the present study does not allow claiming firm conclusions concerning the behavior during cooling. For all samples, the final shear modulus differed from the initial value showing that heating bovine liver tissues above 45 °C generates irreversible stiffness changes. Very few papers have already studied the thermal effects on the elastic properties of liver tissues. However, thermal changes in the complex Young's modulus of porcine livers, assessed by mechanical dynamic compression tests, were previously observed at 60 °C (Kiss *et al* 2009).

The modulus of compression (K) is not expected to be affected by heating, so changes of Young's modulus correspond to changes of shear modulus.

Secondly, the effects of temperature on seven bovine muscle samples (rump roast beef) were quantified. Heating bovine muscular tissues induced a linear decrease of the shear modulus up to 45 °C, with a small change of the slope at 37 °C, then the shear modulus exponentially decreased up to 57 °C and finally exponentially increased. The global stiffness changes are consistent with previous studies (Kruse *et al* 2000, Wu *et al* 2001) (same rate of decrease -1.4 kPa °C^{-1} with an initial shear modulus equal to 70 kPa), but they are not linear contrary to Wu *et al* 's previous observations with MRE (2001). This difference is due to the frame rate of the imaging techniques that here enables the assessment of more subtle changes: one assessment per minute in the present study (real time frame rate could be provided using the SSI technique but would result in huge data sets) versus one assessment every 5 min with MRE. One should also note that the shear wave frequency is different for the two elastography modalities (500 Hz with MRE versus bandwidth of 100 Hz to 400 Hz with SSI).

The linear decrease of stiffness up to 60 °C was previously explained by collagen unfolding and the increase of stiffness above 60 °C was explained by collagen denaturation (Wu *et al* 2001). Obviously, intermediate changes are observed in the present study that cannot be explained by collagen denaturation. These changes could be explained by other proteins' denaturation processes that were listed in previous studies.

4.3. Proteins in muscles

There are three different types of proteins in muscles (Tornberg 2005). First, myofibrillar proteins represent 50 to 55% of the protein content of muscles. These proteins especially include myofilamentous fibrous proteins myosin (alpha-helical structure) and actin. Then, sarcoplasmic proteins (mainly globular proteins) represent 30 to 35% of the protein content. Finally, collagen located in the connective tissues represents 10 to 15% of the protein content. Collagen is a specific 3D triple helix stabilized by H-bonds.

All these proteins are modified by heating. Above 30 °C, myosin and collagen unfold. Then, sarcoplasmic proteins aggregate between 40 °C and 60 °C (Hamm 1977, Tornberg 2005), which leads to the destruction of cell membranes and consequently to myosin aggregation (Tornberg 2005, Xiong and Brekke 1990). Following myosin aggregation, myosin gelation begins at about 45 °C (Tornberg 2005, Xiong and Brekke 1990). Above 53 °C, collagen H-Bonds are broken and consequently collagen is modified from the 3D-helical state to a random-like structure (Tornberg 2005, Wright and Humphrey 2002). In parallel, longitudinal shrinkage of myofibrils is observed because of myosin gelation and the absence of membranes constraints (Tornberg 2005). Finally, sarcoplasmic proteins gelation and longitudinal shrinkage of collagen fibers are observed above 60 °C (Lepetit 2007, 2008, Tornberg 2005, Wright and Humphrey 2002, Wu *et al* 2001). Thus, at 60 °C, all the proteins, excepted actin, are denatured.

4.4. Protein denaturation and changes of tissue stiffness

By reporting the theoretical temperatures of protein denaturation (Tornberg 2005) on the graph that represents the variation of the shear modulus with temperature, the phases that were identified for the shear modulus variations could be explained (figure 8). One should note that this is a descriptive and an associative study.

- First phase (25–37 °C): the shear modulus linearly decreases due to the myosin and collagen unfolding process, which tends to soften the medium.

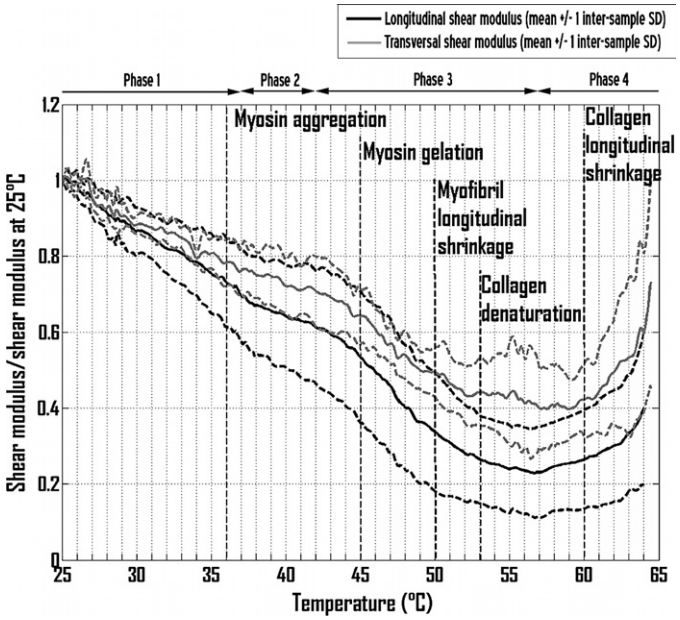

Figure 8. Thermal changes of the longitudinal and transversal shear moduli of bovine muscle and comparison with theoretical temperature thresholds of protein denaturation (Tornberg 2005).

- Second phase (37–43 °C): the shear modulus linearly decreases at a rate slightly smaller. This can be explained by the beginning of myosin aggregation, which tends to stiffen the medium.
- Third phase (43–57 °C): the shear modulus exponentially decreases. At the beginning, the shear modulus hugely decreases with temperature, which can be explained by myosin gelation that is known to soften the medium. In contrast, the shrinkage of myofibrils and collagen denaturation tends to stiffen the media, so that the shear modulus is stabilized at the end of this phase.
- Last phase (above 57 °C): the shear modulus increases due to the combined effect of myofibrilar shrinkage and collagen shrinkage which both stiffen the medium.

4.5. Effect of anisotropy

Before heating, the transversal shear modulus was 1.80 ± 0.19 times smaller than the longitudinal one, which is consistent with previous studies (Kruse *et al* 2000, Wu *et al* 2001) and anatomical knowledge.

To our knowledge, this study is the first that describes in detail the temperature dependence of the transversal shear modulus of bovine tissues. The stiffness changes perpendicular to the fibers (transversal shear modulus) were similar to those along the fibers (longitudinal shear modulus). However, the rate of linear decrease is slightly smaller than the one noted for the longitudinal shear modulus ($-2.0\%\ ^\circ C^{-1}$ versus $-2.5\%\ ^\circ C^{-1}$), probably because myofibrils are constrained by the neighboring ones in that direction. Furthermore, the change of slope at 37 °C due to myosin aggregation is not visible perpendicular to fibers.

4.6. Cool down behavior

The behavior of muscular tissues during cooling is driven by the shear modulus at the end of the heating; if it was at least equal to 86% of the initial value (shear modulus at 25 °C, before heating), muscular tissues were stiffened during cooling, but if it was smaller than 81% of the initial shear modulus, the shear modulus was stable during cooling. This original pattern was reproducible and was observed in both the longitudinal and the transversal plane. To better explain this pattern, two additional experiments, made on one muscle, revealed that it did not depend on the maximal temperature, which was the same between the two samples, but it depended on heating duration. Thus, with these conditions of time and temperature, and for the samples that reached a shear modulus at the end of the heating that was smaller than 81% of the initial value, there were probably not enough H-bonds broken to change the structure of the connective tissues. In contrast, for the samples that reached 86% of the initial stiffness, the rate of collagen denaturation may be sufficient to change the structure of the connective tissues and make the whole sample free to shrink.

4.7. Reversibility/irreversibility of stiffness changes

To identify temperature thresholds for irreversible changes of stiffness during heating, four samples were submitted to successive warm up and cool down cycles, from 20 °C to 70 °C. For half of the samples, the coordinates of the point at the end of each cycle were approximately the same up to 62 °C, showing that stiffness changes were reversible in this region, which was already noted in the literature (Wu *et al* 2001). But in contrast, for half of the samples, the final stiffness significantly differed from the initial value after heating at 49 °C and return at 25 °C. Hence, irreversible changes can occur for temperatures between 40 °C and 49 °C, which is probably due to myosin gelation. For all the samples, the evolution of the shear modulus clearly changes above 62 °C, which corresponds to collagen denaturation (Lepetit *et al* 2000, Wall *et al* 1999, Wright and Humphrey 2002). The heating and cooling curves were different, which is typical of viscoelastic media. Moreover, the area between the two curves increased with increasing temperature up to 49 °C, showing that the entropy of the system was increasing during heating. This phenomenon was previously noted for rubber-like materials (Lawton 1954), but this is, to our knowledge, the first illustration of the phenomenon for muscular tissue.

4.8. Relationship between tissue stiffness and thermal dose

It has been well documented that multiple combinations of time and temperature conditions could reach to the same thermal injuries of tissues (Chen and Humphrey 1998, Dewey 1994, Dewhirst *et al* 2003). Especially, the heating time would logically decrease with increasing temperature to reach thermal isoeffects. To take into account the combined effects of temperature and time, Sapareto and Dewey (1984) proposed an empiric scale of time representing the time of heating at 43 °C (CEM 43 °C), which was latter used to express safety criteria for clinical hyperthermia treatments.

Four samples were heated with different temperature and time conditions. The temperatures of heating were chosen in the range of temperatures for hyperthermia (48 °C, 50.5 °C, 51.5 °C and 55 °C) and the heating duration was chosen to reach cumulative thermal doses ten to hundred times bigger than the threshold of muscular tissue necrosis (Meshorer *et al* 1983).

Of particular interest is the relationship found between the changes of tissue stiffness and the thermal dose: the stiffness changes as a function of the thermal dose were the same for all

the samples, even if the time profile of temperature was very different for each experiment. This confirms the time–temperature equivalency principle for *ex vivo* tissue stiffness. First, the shear modulus linearly decreased up to 20 min probably due to myosin and collagen unfolding processes, then it collapsed from 20 min to 5000 min which may correspond to myosin gelation, and finally it was stabilized until the end of the experiment (figure 7). As stiffness does not increase at the end of the experiments, collagen denaturation seems not to appear in spite of high thermal doses. However, the experiments presented in figure 7 were performed at temperatures below 60 °C which is the temperature threshold for collagen denaturation (Tornberg 2005). Thus, absolute temperature thresholds may have to be reached independently of the heating time to denaturate proteins. Unfortunately, it was not possible to impose a 60 °C temperature constraint in a very short time (9 s) using our experimental setup to achieve the targeted thermal dose. Of course, one should also keep in mind that the present study was conducted *in vitro* so that the concept of thermal dose linked to cellular death is rather meaningless.

Effect of fluid transfers on tissue elasticity. Blood and fat loss as well as water perfusion in the sample were found not to bias or delay the thermal injury of the tissue. Indeed, an experiment was conducted to quantify if potential transfers of fluids between the sample and the surrounding saline bath could affect stiffness during the experiment. Two samples extracted from one bovine muscle were heated and cooled down, one was placed directly into the saline bath as explained in section 2 and the other was placed into a hermetic plastic box. It was observed that fluid loss (blood and fat) increased above 50 °C. Stiffness changes with heating were slightly different between the two samples, especially the decrease rates were different between 25 °C and 43 °C (-0.01% °C^{-1} into water versus -0.02% °C^{-1} into the box), but the difference was smaller than the spatial variance, so that the contact with water does not significantly influence stiffness changes with temperature.

To conclude, the study provides significant improvement in the description of thermal effects on soft tissues mechanical properties. In particular, thermal effects on stiffness were shown to be completely different between liver tissue and muscular tissue of bovines. Changes in liver stiffness are observed only after a temperature threshold ($T > 45$ °C). In contrast, thermal effects on muscle stiffness are much more complex. A descriptive and associative model, which takes into account tissue anisotropy, is proposed in this study, based on the thermal effects on muscular proteins reported in the literature. A significant decrease of muscle stiffness is induced even by low-temperature hyperthermia regimes. In this low temperature range ($T < 43$ °C), stiffness changes are found to be reversible and linear, with a slope linked to tissue-dependent parameters. Between 43 °C and 60 °C, stiffness decreases but its variation is not linear anymore, and irreversible stiffness changes may occur due to myosin gelation. Finally, above 60 °C, a strong irreversible increase of stiffness is observed, corresponding to collagen denaturation. After a 6 h long heating and cooling process, the final tissue stiffness could be either smaller or bigger than the initial one, depending on the stiffness at the end of the heating. Another important result is that, for temperatures between 48 °C and 55 °C, the stiffness changes are directly linked to the cumulative thermal dose. Blood and fat loss and water diffusion through the medium were found to have no effect on the changes of stiffness with temperature. These patterns should be confirmed with experimental conditions closer to the clinical HIFU treatments (local thermal effects, *in vivo* conditions, human tissues). However, the study shows that ultrasound-based quantitative elastography is sensitive to protein denaturation which gives promising prospects for the prediction and monitoring of thermal effects on tissues using ultrasound. Finally, the stiffness changes as a function of the thermal dose were the same for all samples, even if the time profile of

temperature was very different for each experiment. This confirms the time–temperature equivalency principle for *ex vivo* tissue stiffness. It also emphasizes that elasticity monitoring could play a key role in the development of ultrasound-guided HIFU systems.

Acknowledgment

The authors gratefully acknowledge Marc Borg for his contribution to the experiments on liver tissues. Mathias Fink and Mickael Tanter are co-founders and shareholders of Supersonic Imagine.

References

Anan A and Kaczkowski J P 2008 Noninvasive measurement of local thermal diffusivity using backscattered ultrasound and focused ultrasound heating *Ultrasound Med. Biol.* **34** 1449–64

Apter J T 1972 Influence of composition on thermal properties of tissues *Biomechanics. Its Foundations and Objectives* ed Y C Fung, N Perrone and M Anliker (London: Prentice-Hall) pp 217–35

Bercoff J, Pernot M, Tanter M and Fink M 2004a Monitoring thermally-induced lesions with supersonic shear imaging *Ultrason. Imaging* **26** 71–84

Bercoff J, Tanter M and Fink M 2004b *S*upersonic shear imaging: a new technique for soft tissue elasticity mapping *IEEE Trans. Ultrason. Ferroelectr. Freq. Control* **51** 396–409

Chen S S and Humphrey J D 1998 Heat-induced changes in the mechanics of a collagenous tissue: pseudoelastic behavior at 37 °C *J. Biomech.* **31** 211–6

Cline H E, Hynynen K, Hardy C J, Watkins R D, Schenck J F and Jolesz F A 1994 MR temperature mapping of focused ultrasound surgery *Magn. Reson. Med.* **31** 628–36

Curiel L, Chopra R and Hynynen K 2009 *In vivo* monitoring of focused ultrasound surgery using local harmonic motion *Ultrasound Med. Biol.* **35** 65–78

Dewey W C 1994 Arrhenius relationships from the molecule and cell to the clinic *Int. J. Hyperth.* **10** 457–83

Dewhirst M W, Viglianti B L, Lora-Michiels M, Hanson M and Hoopes P J 2003 Basic principles of thermal dosimetry and thermal thresholds for tissue damage from hyperthermia *Int. J. Hyperth.* **19** 267–94

Hamm R 1977 Changes of muscle proteins during the heating of meat *Physical, Chemical and Biological Changes in Food Caused by Thermal Processing* ed T Höyem and O Kvale (London: Applied Science Publishing) pp 101–34

Kiss M Z, Daniels M J and Varghese T 2009 Investigation of temperature-dependent viscoelastic properties of thermal lesions in *ex vivo* animal liver tissue *J. Biomech.* **42** 959–66

Kruse S A, Smith J A, Lawrence A J, Dresner M A, Manduca A, Greenleaf J and Ehman R 2000 Tissue characterization using magnetic resonance elastography: preliminary results *Phys. Med. Biol.* **6** 1579–90

Lawton R W 1954 The thermoelastic behavior of isolated aortic strips of the dog *Circ. Res.* **11** 344–53

Lepetit J 2007 A theoretical approach of the relationships between collagen content, collagen cross-links and meat tenderness *Meat Sci.* **76** 147–59

Lepetit J 2008 Collagen contribution to meat toughness: theoretical aspects *Meat Sci.* **80** 960–7

Lepetit J, Grajales A and Favier R 2000 Modelling the effect of sarcomere length on collagen thermal shortening in cooked meat: consequence on meat toughness *Meat Sci.* **54** 239–50

Maass-Moreno R, Damianou C A and Sanghvi N T 1996 Noninvasive temperature estimation in tissue via ultrasound echo-shifts: Part II. *In vitro* study *J. Acoust. Soc. Am.* **100** 2522–30

Meshorer A, Prionas S D, Fajardo L F, Meyer J L, Hahn G M and Martinez A A 1983 The effects of hyperthermia on normal mesenchymal tissues. Application of a histologic grading system *Arch. Pathol. Lab. Med.* **107** 328–34

Miller N R, Bamber J C and Meaney P M 2002 Fundamental limitations of noninvasive temperature imaging by means of ultrasound echo strain estimation *Ultrasound Med. Biol.* **28** 1319–33

Muller M, Gennisson J-L, Deffieux T, Tanter M and Fink M 2009 Quantitative viscoelasticity mapping of human liver using supersonic shear imaging: preliminary *in vivo* feasibility study *Ultrasound Med. Biol.* **35** 219–29

Ophir J, Céspedes I, Ponnekanti H, Yasdi Y and Li X 1991 Elastography: a quantitative method for imaging the elasticity of biological tissues *Ultrason. Imaging* **13** 111–34

Pernot M, Tanter M, Bercoff J, Waters K R and Fink M 2004 Temperature estimation using ultrasonic spatial compound imaging *IEEE Trans. Ultrason., Ferroelectr. Freq. Control* **51** 606–15

Rieke V and Pauly K B 2008 MR thermometry *J. Magn. Reson. Imaging* **27** 376–90

Sapareto S A and Dewey W C 1984 Thermal dose determination in cancer therapy *Int. J. Radiat. Oncol. Biol. Phys.* **10** 787–800

Seip R and Ebbini E S 1995 Non invasive estimation of tissue temperature response to heating fields using diagnostic ultrasound *IEEE Trans. Biomed. Eng.* **42** 828–39

Simon C, Vanbaren P and Ebbini E S 1998 Two-dimensional temperature estimation using diagnostic ultrasound *IEEE Trans. Ultrason. Ferroelectr. Freq. Control* **45** 1088–99

Tanter M, Bercoff J, Athanasiou A, Deffieux T, Gennisson J-L, Montaldo G, Muller M, Tardivon A and Fink M 2008 Quantitative assessment of breast lesion viscoelasticity: initial clinical results using supersonic shear imaging *Ultrasound Med. Biol.* **34** 1373–86

Tornberg E 2005 Effects of heat on meat proteins—implications on structure and quality of meat products *Meat Sci.* **70** 493–508

Wall M S, Deng X-H, Torzilli P A, Doty S B, O'Brien S J and Warren R F 1999 Thermal modification of collagen *J. Shoulder Elbow Surg.* **8** 339–44

Wright N T and Humphrey J D 2002 Denaturation of collagen via heating: an irreversible rate process *Annu. Rev. Biomed. Eng.* **4** 109–28

Wu T, Felmlee J, Greenleaf J, Riederer S and Ehman R 2001 Assessment of thermal tissue ablation with MR elastography *Magn. Reson. Med.* **45** 80–7

Xiong Y L and Brekke C J 1990 Thermal transitions of salt-soluble proteins from pre- and postrigor chicken muscles *J. Food Sci.* **55** 1540–3